

Simple renormalizable flavor symmetry for neutrino oscillationsY. H. Ahn,^{*} Seungwon Baek,[†] and Paolo Gondolo[‡]*School of Physics, KIAS, Seoul 130-722, Korea*

(Received 26 July 2012; published 10 September 2012)

The recent measurement of a nonzero neutrino mixing angle θ_{13} requires a modification of the tri-bimaximal mixing pattern that predicts a zero value for it. We propose a new neutrino mixing pattern based on a spontaneously broken A_4 flavor symmetry and a type-I seesaw mechanism. Our model allows for approximate tri-bimaximal mixing and nonzero θ_{13} , and contains a natural way to implement low- and high-energy CP violations in neutrino oscillations, and leptogenesis with a renormalizable Lagrangian. Both normal and inverted mass hierarchies are permitted within 3σ experimental bounds, with the prediction of small (large) deviations from maximality in the atmospheric mixing angle for the normal (inverted) case. Interestingly, we show that the inverted case is excluded by the global analysis in 1σ experimental bounds, while the most recent MINOS data seem to favor the inverted case. Our model make predictions for the Dirac CP phase in the normal and inverted hierarchies, which can be tested in near-future neutrino oscillation experiments. Our model also predicts the effective mass $|m_{ee}|$ measurable in neutrinoless double beta decay to be in the range $0.04 \leq |m_{ee}| \leq 0.15$ eV for the normal hierarchy and $0.06 \leq |m_{ee}| \leq 0.11$ eV for the inverted hierarchy, both of which are within the sensitivity of the next generation experiments.

DOI: [10.1103/PhysRevD.86.053004](https://doi.org/10.1103/PhysRevD.86.053004)

PACS numbers: 11.30.Hv, 14.60.Pq

INTRODUCTION

The large values of the solar ($\theta_{12} \simeq 35^\circ$) and atmospheric ($\theta_{23} \simeq 45^\circ$) [1] neutrino mixing angles may be telling us about new symmetries in the lepton sector not present in the quark sector, and may provide us with a clue to the nature of the quark-lepton physics beyond the standard model. Theoretically, a great deal of effort has been put into constructing flavor models with high predictive power, especially those giving the tri-bimaximal (TBM) mixing angles [2]:

$$\begin{aligned} \theta_{13} &= 0, & \theta_{23} &= \frac{\pi}{4} = 45^\circ, \\ \theta_{12} &= \sin^{-1}\left(\frac{1}{\sqrt{3}}\right) \simeq 35.3^\circ. \end{aligned} \quad (1)$$

However, the Daya Bay and RENO collaborations [3,4] have reported the first measurements of a nonzero value for the mixing angle θ_{13} :

$$\sin^2 2\theta_{13} = 0.092 \pm 0.016(\text{stat}) \pm 0.005(\text{syst}), \quad (2)$$

and

$$\sin^2 2\theta_{13} = 0.113 \pm 0.013(\text{stat}) \pm 0.019(\text{syst}), \quad (3)$$

respectively, corresponding to an angle $\theta_{13} \approx 9^\circ$. These results are in good agreement with the previous data from the T2K, MINOS and Double Chooz collaborations [5]. A nonzero value of θ_{13} indicates that the TBM pattern for neutrino mixing should be modified. In addition, at the

Neutrino 2012 conference in Kyoto, the MINOS Collaboration has announced a nonmaximal value for the atmospheric mixing angle θ_{23} [6],

$$\sin^2 2\theta_{23} = 0.94_{-0.05}^{+0.04} \pm 0.04, \quad (4)$$

with maximal mixing disfavored at the 88% C.L. This result, which was not included the global analysis in Ref. [7], comes from the analysis of ν_μ disappearance in the MINOS accelerator beam, and points to one of two possible values for θ_{23} , namely $\theta_{23} = 38^\circ$ or $\theta_{23} = 52^\circ$. If it holds, this result also calls for a deviation from the TBM mixing pattern.

Furthermore, the presence of CP violation in the lepton sector is still unknown. Experimentally, CP violation may become observable in a future generation of neutrino oscillation experiments (T2K, NO ν A) [8]. Theoretically, a flavor symmetry that describes and explains the large reactor mixing angle $\theta_{13} \simeq 9^\circ$ while keeping the TBM values $\theta_{23} \simeq 45^\circ$ and $\theta_{12} \simeq 35^\circ$ may originate in two ways: (i) a large $\theta_{13} = \lambda_C/\sqrt{2}$, with λ_C the Cabibbo angle, mainly governed by higher-order corrections in the charged lepton sector [9], where the TBM pattern is a good zero-order approximation to reality, or (ii) a large θ_{13} from the neutrino sector itself through a new flavor symmetry without resorting to higher-order corrections in the charged lepton sector [10].

In this paper, we propose a new and simple model for the lepton sector with A_4 flavor symmetry in the framework of a type-I seesaw mechanism. It is different from previous works using A_4 flavor symmetries [11–14]¹ in that the Dirac neutrino Yukawa coupling constants do not all have the same

^{*}yhahn@kias.re.kr[†]swbaek@kias.re.kr[‡]On sabbatical leave from the University of Utah. paolo.gondolo@utah.edu¹Ma and Rajasekaran [15] have introduced for the first time the A_4 symmetry to avoid the mass degeneracy of μ and τ under a μ - τ symmetry [16].

magnitude. Our model can naturally explain the TBM large value of θ_{13} and can also provide a possibility for low-energy CP violation in neutrino oscillations with a renormalizable Lagrangian and small Yukawa coupling parameters, i.e., neutrino masses. The seesaw mechanism, besides explaining of smallness of the measured neutrino masses, has another appealing feature: generating the observed baryon asymmetry in our Universe by means of leptogenesis [17]. Since the conventional A_4 models realized with type-I or -III seesaw and a tree-level Lagrangian lead to an exact TBM and vanishing leptonic CP -asymmetries responsible for leptogenesis (due to the proportionality of the $Y_\nu^\dagger Y_\nu$ combination of the Dirac neutrino Yukawa matrix Y_ν to the unit matrix), authors usually introduce soft-breaking terms or higher-dimensional operators with many parameters, in order to explain the nonzero θ_{13} as well as the nonvanishing CP -asymmetries.

Our model is based on a renormalizable $SU(2)_L \times U(1)_Y \times A_4$ Lagrangian with minimal Yukawa couplings, and gives rise to a nondegenerate Dirac neutrino Yukawa matrix and a unique CP -violation pattern. This opens the possibility of explaining the nonzero value of $\theta_{13} \simeq 9^\circ$ still maintaining TBM for the other two neutrino mixing angles $\theta_{23} \simeq 45^\circ$ and $\theta_{12} \simeq 35^\circ$; furthermore, this allows an economic way to achieve low-energy CP violation in neutrino oscillations as well as high-energy CP violation for leptogenesis.

This paper is organized as follows. In the next section, we lay down the particle content and the field representations under the A_4 flavor symmetry in our model, as well as explain the characteristic points of our model phenomenology at low and high energy. In Sec. III, we present the neutrino mixing angles, and how the low-energy CP violation could be generated in both normal and inverted mass hierarchies, including our predictions for neutrinoless double beta decay. We give our conclusions in Sec. IV, and in Appendix A we outline the minimization of the scalar potential and the vacuum alignments.

II. FLAVOR A_4 SYMMETRY FOR NONZERO θ_{13} AND LEPTOGENESIS

In the absence of flavor symmetries, particle masses and mixings are generally undetermined in a gauge theory. Here, to understand the present nonzero θ_{13} and TBM angles (θ_{12}, θ_{23}) of the neutrino oscillation data and baryogenesis via leptogenesis, we propose a new discrete symmetry based on an A_4 flavor symmetry for leptons in a renormalizable Lagrangian.²

The group A_4 is the symmetry group of the tetrahedron, isomorphic to the finite group of the even permutations of four objects. The group A_4 has two generators, denoted S and T , satisfying the relations $S^2 = T^3 = (ST)^3 = 1$.

²To include the quark sector, the symmetry could be promoted to the binary tetrahedral group T' [18].

In the three-dimensional real representation, S and T are given by

$$S = \begin{pmatrix} 1 & 0 & 0 \\ 0 & -1 & 0 \\ 0 & 0 & -1 \end{pmatrix}, \quad T = \begin{pmatrix} 0 & 1 & 0 \\ 0 & 0 & 1 \\ 1 & 0 & 0 \end{pmatrix}. \quad (5)$$

A_4 has four irreducible representations: one triplet $\mathbf{3}$ and three singlets $\mathbf{1}, \mathbf{1}', \mathbf{1}''$. An A_4 triplet (a_1, a_2, a_3) transforms in the unitary representation by multiplication with the S and T matrices in Eq. (5) above,

$$S \begin{pmatrix} a_1 \\ a_2 \\ a_3 \end{pmatrix} = \begin{pmatrix} a_1 \\ -a_2 \\ -a_3 \end{pmatrix}, \quad T \begin{pmatrix} a_1 \\ a_2 \\ a_3 \end{pmatrix} = \begin{pmatrix} a_2 \\ a_3 \\ a_1 \end{pmatrix}. \quad (6)$$

An A_4 singlet a is invariant under the action of S ($Sa = a$), while the action of T produces $Ta = a$ for $\mathbf{1}$, $Ta = \omega a$ for $\mathbf{1}'$, and $Ta = \omega^2 a$ for $\mathbf{1}''$, where $\omega = e^{i2\pi/3}$ is a complex cubic root of unity. Products of two A_4 representations decompose into irreducible representations according to the following multiplication rules: $\mathbf{3} \otimes \mathbf{3} = \mathbf{3}_s \oplus \mathbf{3}_a \oplus \mathbf{1} \oplus \mathbf{1}' \oplus \mathbf{1}''$, $\mathbf{1}' \otimes \mathbf{1}'' = \mathbf{1}$, $\mathbf{1}' \otimes \mathbf{1}' = \mathbf{1}''$ and $\mathbf{1}'' \otimes \mathbf{1}'' = \mathbf{1}'$. Explicitly, if (a_1, a_2, a_3) and (b_1, b_2, b_3) denote two A_4 triplets,

$$\begin{aligned} (a \otimes b)_{\mathbf{3}_s} &= (a_2 b_3 + a_3 b_2, a_3 b_1 + a_1 b_3, a_1 b_2 + a_2 b_1), \\ (a \otimes b)_{\mathbf{3}_a} &= (a_2 b_3 - a_3 b_2, a_3 b_1 - a_1 b_3, a_1 b_2 - a_2 b_1), \\ (a \otimes b)_{\mathbf{1}} &= a_1 b_1 + a_2 b_2 + a_3 b_3, \\ (a \otimes b)_{\mathbf{1}'} &= a_1 b_1 + \omega a_2 b_2 + \omega^2 a_3 b_3, \\ (a \otimes b)_{\mathbf{1}''} &= a_1 b_1 + \omega^2 a_2 b_2 + \omega a_3 b_3. \end{aligned} \quad (7)$$

To make the presentation of our model physically more transparent, we define the T -flavor quantum number T_f through the eigenvalues of the operator T , for which $T^3 = 1$. In detail, we say that a field f has T -flavor $T_f = 0, +1$, or -1 when it is an eigenfield of the T operator with eigenvalue $1, \omega, \omega^2$, respectively (in short, with eigenvalue ω^{T_f} for T -flavor T_f , considering the cyclical properties of the cubic root of unity ω). The T -flavor is an additive quantum number modulo 3. We also define the S -flavor-parity through the eigenvalues of the operator S , which are $+1$ and -1 since $S^2 = 1$, and we speak of S -flavor-even and S -flavor-odd fields. For A_4 -singlets, which are all S -flavor-even, the $\mathbf{1}$ representation has no T -flavor ($T_f = 0$), the $\mathbf{1}'$ representation has T -flavor $T_f = +1$, and the $\mathbf{1}''$ representation has T -flavor $T_f = -1$. Since for A_4 -triplets, the operators S and T do not commute, A_4 -triplet fields cannot simultaneously have a definite T -flavor and a definite S -flavor-parity. While the real representation of A_4 in Eqs. (5), in which S is diagonal, is useful in writing the Lagrangian, the physical meaning of our model is more apparent in the T -flavor representation in which T is diagonal. This representation is obtained through the unitary transformation

$$A \rightarrow A' = U_\omega A U_\omega^\dagger, \quad (8)$$

where A is any A_4 matrix in the real representation and

$$U_\omega = \frac{1}{\sqrt{3}} \begin{pmatrix} 1 & 1 & 1 \\ 1 & \omega^2 & \omega \\ 1 & \omega & \omega^2 \end{pmatrix}. \quad (9)$$

We have

$$S' = \frac{1}{3} \begin{pmatrix} -1 & 2 & 2 \\ 2 & -1 & 2 \\ 2 & 2 & -1 \end{pmatrix}, \quad T' = \begin{pmatrix} 1 & 0 & 0 \\ 0 & \omega & 0 \\ 0 & 0 & \omega^2 \end{pmatrix}. \quad (10)$$

Despite the physical advantages of the S' , T' representation, for clarity of exposition and to avoid confusion and complications, in this paper we use the real representation S , T almost exclusively. For reference, an A_4 triplet field with components (a_1, a_2, a_3) in the real representation can be expressed in terms of T -flavor eigenfields (a_e, a_μ, a_τ) (the notation comes from our lepton assignments below) as

$$\begin{aligned} a_1 &= \frac{a_e + a_\mu + a_\tau}{\sqrt{3}}, \\ a_2 &= \frac{a_e + \omega^2 a_\mu + \omega a_\tau}{\sqrt{3}}, \\ a_3 &= \frac{a_e + \omega a_\mu + \omega^2 a_\tau}{\sqrt{3}}. \end{aligned} \quad (11)$$

Inversely,

$$\begin{aligned} a_e &= \frac{a_1 + a_2 + a_3}{\sqrt{3}}, \\ a_\mu &= \frac{a_1 + \omega a_2 + \omega^2 a_3}{\sqrt{3}}, \\ a_\tau &= \frac{a_1 + \omega^2 a_2 + \omega a_3}{\sqrt{3}}. \end{aligned} \quad (12)$$

We extend the standard model (SM) by the inclusion of an A_4 -triplet of right-handed $SU(2)_L$ -singlet Majorana neutrinos N_R , and the introduction of two types of scalar Higgs fields besides the usual SM $SU(2)_L$ -doublet Higgs bosons Φ , which we take to be an A_4 -singlet with no T -flavor ($\mathbf{1}$ representation): a second $SU(2)_L$ -doublet of Higgs bosons η , which is distinguished from Φ by being an A_4 -triplet, and an $SU(2)_L$ -singlet A_4 -triplet real scalar field χ :

$$\Phi = \begin{pmatrix} \varphi^+ \\ \varphi^0 \end{pmatrix}, \quad \eta_j = \begin{pmatrix} \eta_j^+ \\ \eta_j^0 \end{pmatrix}, \quad \chi_j, \quad j = 1, 2, 3. \quad (13)$$

We assign each flavor of leptons to one of the three A_4 singlet representations: the electron flavor to the $\mathbf{1}$ (T -flavor 0), the muon flavor to the $\mathbf{1}'$ (T -flavor +1), and the tau flavor to the $\mathbf{1}''$ (T -flavor -1). (Note in this respect that our A_4 flavor group is not a symmetry under exchange of any two lepton flavors, like e and μ , for example. Our A_4 flavor group is implemented as a global symmetry of the Lagrangian, later spontaneously broken, but some fields are not invariant under A_4 transformations, much in the same way as the implementation of $SU(2)_L \times U(1)_Y$ in the SM, where left-handed and right-handed fermions are assigned to different representations of the gauge group.) Then we take the usual Higgs boson doublet Φ to be invariant under A_4 , that is to be a flavor-singlet $\mathbf{1}$ with no T -flavor. The other Higgs doublet η , the Higgs singlet χ , and the singlet neutrinos N_R are assumed to be triplets under A_4 , and can so be used to introduce lepton-flavor violation in an A_4 symmetric Lagrangian.

The field content of our model and the field assignments to $SU(2)_L \times U(1)_Y \times A_4$ representations are summarized in Table I. These representation assignments and the requirement that the Lagrangian be renormalizable and A_4 -symmetry forbid the presence of tree-level leptonic flavor-changing charged currents.

The renormalizable Yukawa interactions in the neutrino and charged lepton sectors invariant under $SU(2)_L \times U(1)_Y \times A_4$ are (including a Majorana mass term for the right-handed neutrinos)

$$\begin{aligned} -\mathcal{L}_{\text{Yuk}} &= y_1^e \bar{L}_e (\tilde{\eta} N_R)_{\mathbf{1}} + y_2^\mu \bar{L}_\mu (\tilde{\eta} N_R)_{\mathbf{1}'} + y_3^\tau \bar{L}_\tau (\tilde{\eta} N_R)_{\mathbf{1}''} \\ &+ \frac{1}{2} M (\bar{N}_R^c N_R)_{\mathbf{1}} + \frac{1}{2} y_R^e (\bar{N}_R^c N_R)_{\mathbf{3}, \chi} + y_e \bar{L}_e \Phi e_R \\ &+ y_\mu \bar{L}_\mu \Phi \mu_R + y_\tau \bar{L}_\tau \Phi \tau_R + \text{H.c.}, \end{aligned} \quad (14)$$

where $\tilde{\eta} \equiv i\tau_2 \eta^*$ and τ_2 is a Pauli matrix. In this Lagrangian, each flavor of neutrinos and each flavor of charged leptons has its own independent Yukawa term, since they belong to different singlet representations $\mathbf{1}$, $\mathbf{1}'$, and $\mathbf{1}''$ of A_4 : the neutrino Yukawa terms involve the A_4 -triplets η and N_R , which combine into the appropriate singlet representation; the charged-lepton Yukawa terms involve the A_4 -singlet Φ and the A_4 -singlet right-handed charged-leptons e_R , μ_R , and τ_R . The right-handed neutrinos have an additional Yukawa term that involves the A_4 -triplet

TABLE I. Representations of the fields under A_4 and $SU(2)_L \times U(1)_Y$.

| Field | L_e, L_μ, L_τ | e_R, μ_R, τ_R | N_R | χ | Φ | η |
|-------------------------|---|---|--------------|--------------|--------------------|--------------------|
| A_4 | $\mathbf{1}, \mathbf{1}', \mathbf{1}''$ | $\mathbf{1}, \mathbf{1}', \mathbf{1}''$ | $\mathbf{3}$ | $\mathbf{3}$ | $\mathbf{1}$ | $\mathbf{3}$ |
| $SU(2)_L \times U(1)_Y$ | $(2, -\frac{1}{2})$ | $(1, -1)$ | $(1, 0)$ | $(1, 0)$ | $(2, \frac{1}{2})$ | $(2, \frac{1}{2})$ |

SM-singlet Higgs χ . The mass term $\frac{1}{2}M(\bar{N}_R^c N_R)_1$ for the right-handed neutrinos is necessary to implement the seesaw mechanism by making the right-handed neutrino mass parameter M large.

The Higgs potential of our model contains many terms and is listed in Appendix A, Eqs. (A1)–(A7).³ We spontaneously break the A_4 flavor symmetry by giving nonzero vacuum expectation values to some components of the A_4 -triplets χ and η . As seen in Appendix A, the minimization of our scalar potential gives the following vacuum expectation values (VEVs), all real:

$$\begin{aligned} \langle \varphi^0 \rangle &= \frac{v_\Phi}{\sqrt{2}} \neq 0, & \langle \eta_1^0 \rangle &= \langle \eta_2^0 \rangle = \langle \eta_3^0 \rangle \equiv \frac{v_\eta}{\sqrt{2}} \neq 0, \\ \langle \chi_1 \rangle &\equiv v_\chi \neq 0, & \langle \chi_2 \rangle &= \langle \chi_3 \rangle = 0. \end{aligned} \quad (15)$$

The SM VEV $v = (\sqrt{2}G_F)^{-1/2} = 246$ GeV results from the combination $v = \sqrt{v_\Phi^2 + 3v_\eta^2}$. The nonzero expectation value $\langle \varphi^0 \rangle = v_\Phi/\sqrt{2}$ does not break the A_4 symmetry, because the standard model Higgs is A_4 -flavorless. The nonzero expectation value $\langle \eta \rangle = (v_\eta, v_\eta, v_\eta)/\sqrt{2}$ breaks the S -flavor-parity $(\eta_1, \eta_2, \eta_3) \rightarrow (\eta_1, -\eta_2, -\eta_3)$ but leaves the vacuum T -flavor $T_f = 0$. In other words, after η acquires a nonzero VEV, the T -flavor is still conserved but the S -flavor-parity is not. Since η appears only in the Higgs sector and in interactions with the light leptons, we say that the light neutrino sector has a residual Z_3 symmetry expressed by the subgroup $\{1, T, T^2\}$ that leads to the conservation of T -flavor in terms involving mixing with the light neutrinos or interactions with the charged leptons. The nonzero expectation value $\langle \chi \rangle = (v_\chi, 0, 0)$ maintains the S -flavor-parity of the vacuum (it is S -flavor-even) but gives the vacuum the symmetric combination of T -flavors $(a_0 + a_{+1} + a_{-1})/\sqrt{3}$. That is, after χ acquires a nonzero VEV, the S -flavor-parity is conserved but the T -flavor is not. Since χ appears only in the Higgs sector and in interactions with the heavy Majorana neutrinos, we say that the heavy neutrino sector has a residual Z_2 symmetry expressed by the subgroup $\{1, S\}$ leading to the conservation of S -flavor-parity in terms involving mixing or interactions with the heavy Majorana neutrinos.

When a non-Abelian discrete symmetry like our A_4 is considered, it is crucial to check the stability of the vacuum. In the presence of two A_4 -triplet Higgs scalars χ and η , Higgs potential terms involving both χ and η , which would be written as $V(\chi\eta)$ in Eqs. (A1)–(A7), would be problematic for vacuum stability. Such stability problems can be naturally solved, for instance, in the presence of extra dimensions or in supersymmetric dynamical completions

³We note that at TeV-scale the higher-dimensional operators ($d \geq 5$) driven by χ and η fields are suppressed by a cutoff scale Λ which we assume is a very high energy scale, i.e., GUT or Planck scale. And in this paper we neglect the effects of higher-dimensional operators.

[13,19]. In these cases, $V(\chi\eta)$ is not allowed or highly suppressed.

The physical Higgs fields are obtained in the usual way. In the Higgs sector we have four Higgs doublets Φ , η_1 , η_2 and η_3 , and three Higgs singlets χ_1 , χ_2 , and χ_3 . They contain in total 16 degrees of freedom: six charged Higgs fields $\eta_{1,2,3}^\pm$, with $\eta_j^+ \equiv (\eta_j^-)^*$, seven neutral Higgs scalars h , $h_{1,2,3}$, $\chi_{1,2,3}^0$, and three Higgs pseudoscalars $A_{1,2,3}$. We can write, after electroweak- and A_4 -symmetry breaking and minimization of the potential,

$$\begin{aligned} \Phi &= \begin{pmatrix} \varphi^+ \\ \frac{1}{\sqrt{2}}(v_\Phi + h + iA_0) \end{pmatrix}, \\ \chi_1 &= v_\chi + \chi_1^0, \\ \chi_2 &= \chi_2^0, \quad \chi_3 = \chi_3^0, \\ \eta_j &= \begin{pmatrix} \eta_j^+ \\ \frac{1}{\sqrt{2}}(v_\eta + h_j + iA_j) \end{pmatrix}, \quad j = 1, 2, 3. \end{aligned} \quad (16)$$

The action of the residual Z_2 generator S on the physical fields is

$$(N_{R1}, N_{R2}, N_{R3}) \rightarrow (N_{R1}, -N_{R2}, -N_{R3}), \quad (17)$$

$$(\chi_1^0, \chi_2^0, \chi_3^0) \rightarrow (\chi_1^0, -\chi_2^0, -\chi_3^0), \quad (18)$$

$$(h_1, h_2, h_3) \rightarrow (h_1, -h_2, -h_3), \quad (19)$$

$$(A_1, A_2, A_3) \rightarrow (A_1, -A_2, -A_3), \quad (20)$$

$$(\eta_1^+, \eta_2^+, \eta_3^+) \rightarrow (\eta_1^+, -\eta_2^+, -\eta_3^+), \quad (21)$$

all other fields are invariant. The action of the residual Z_3 generator T on the physical fields is [the triplet fields a_1 , a_2 , and a_3 and the triplet fields a_e , a_μ , and a_τ are linear combinations of each other, see Eqs. (11) and (12)]

$$(e, \mu, \tau) \rightarrow (e, \omega\mu, \omega^2\tau), \quad (22)$$

$$(v_e, v_\mu, v_\tau) \rightarrow (v_e, \omega v_\mu, \omega^2 v_\tau), \quad (23)$$

$$(N_{Re}, N_{R\mu}, N_{R\tau}) \rightarrow (N_{Re}, \omega N_{R\mu}, \omega^2 N_{R\tau}), \quad (24)$$

$$(\chi_e^0, \chi_\mu^0, \chi_\tau^0) \rightarrow (\chi_e^0, \omega \chi_\mu^0, \omega^2 \chi_\tau^0), \quad (25)$$

$$(h_e, h_\mu, h_\tau) \rightarrow (h_e, \omega h_\mu, \omega^2 h_\tau), \quad (26)$$

$$(A_e, A_\mu, A_\tau) \rightarrow (A_e, \omega A_\mu, \omega^2 A_\tau), \quad (27)$$

$$(\eta_e^+, \eta_\mu^+, \eta_\tau^+) \rightarrow (\eta_e^+, \omega \eta_\mu^+, \omega^2 \eta_\tau^+), \quad (28)$$

all other fields are invariant.

After electroweak and A_4 symmetry breaking, the neutral Higgs fields acquire vacuum expectation values and

give masses to the charged leptons and neutrinos: the Higgs doublet gives Dirac masses to the charged leptons, the Higgs doublet η gives Dirac masses to the three SM neutrinos, and the Higgs singlet χ gives a Majorana mass to the right-handed neutrino N_R .

The charged lepton mass matrix is automatically diagonal due to the A_4 -singlet nature of the charged lepton and SM-Higgs fields. The right-handed neutrino mass has

$$-\mathcal{L}_m = \frac{v_\Phi}{\sqrt{2}}(y_e \bar{e}_L e_R + y_\mu \bar{\mu}_L \mu_R + y_\tau \bar{\tau}_L \tau_R) + \frac{v_\eta}{\sqrt{2}}\{(y_1^\nu \bar{\nu}_e + y_2^\nu \bar{\nu}_\mu + y_3^\nu \bar{\nu}_\tau)N_{R1} + (y_1^\nu \bar{\nu}_e + y_2^\nu \omega \bar{\nu}_\mu + y_3^\nu \omega^2 \bar{\nu}_\tau)N_{R2} + (y_1^\nu \bar{\nu}_e + y_2^\nu \omega^2 \bar{\nu}_\mu + y_3^\nu \omega \bar{\nu}_\tau)N_{R3}\} + \frac{M}{2}(\bar{N}_{R1}^c N_{R1} + \bar{N}_{R2}^c N_{R2} + \bar{N}_{R3}^c N_{R3}) + \frac{y_R^\nu v_\chi}{2}(\bar{N}_{R2}^c N_{R3} + \bar{N}_{R3}^c N_{R2}) + \text{H.c.} \quad (29)$$

This form shows clearly that the terms in v_η break the S -flavor-parity symmetry (17)–(21), while the other mass terms preserve it. Passing to the T -flavor eigenfields

$$N_{Re} = \frac{N_{R1} + N_{R2} + N_{R3}}{\sqrt{3}}, \quad (30)$$

$$N_{R\mu} = \frac{N_{R1} + \omega N_{R2} + \omega^2 N_{R3}}{\sqrt{3}}, \quad (31)$$

$$N_{R\tau} = \frac{N_{R1} + \omega^2 N_{R2} + \omega N_{R3}}{\sqrt{3}}, \quad (32)$$

with respective T -flavor $T_f = 0, +1, -1$, the lepton mass Lagrangian reads

$$-\mathcal{L}_m = \frac{v_\Phi}{\sqrt{2}}(y_e \bar{e}_L e_R + y_\mu \bar{\mu}_L \mu_R + y_\tau \bar{\tau}_L \tau_R) + v_\eta \sqrt{\frac{3}{2}}(y_1^\nu \bar{\nu}_e N_{Re} + y_2^\nu \bar{\nu}_\mu N_{R\mu} + y_3^\nu \bar{\nu}_\tau N_{R\tau}) + \frac{M}{2}(\bar{N}_{Re}^c N_{Re} + \bar{N}_{R\mu}^c N_{R\mu} + \bar{N}_{R\tau}^c N_{R\tau}) + \frac{y_R^\nu v_\chi}{2}[\bar{N}_{Re}^c N_{Re} + \bar{N}_{R\mu}^c N_{R\mu} + \bar{N}_{R\tau}^c N_{R\tau} - \frac{1}{3}(\bar{N}_{Re}^c + \bar{N}_{R\mu}^c + \bar{N}_{R\tau}^c)(N_{Re} + N_{R\mu} + N_{R\tau})] + \text{H.c.} \quad (33)$$

This form shows clearly that the terms in v_χ break the T -flavor symmetry (22)–(28), while the other mass terms preserve it.

Inspection of the mass terms in Eq. (33) indicates that, with the VEV alignments in Eq. (15), the A_4 symmetry is spontaneously broken to a residual Z_2 symmetry in the heavy Majorana neutrino sector (conservation of S -flavor-parity in terms not involving v_η or $h_{1,2,3}$) and a residual Z_3 symmetry in the Dirac neutrino sector (conservation of T -flavor in terms not involving v_χ or χ_1^0).

The mass terms in Eq. (29) and the charged gauge interactions in the weak eigenstate basis can be written in (block) matrix form as, using $\bar{N}_R^c m_D v_L^c = \bar{\nu}_L m_D^T N_R$,

the (large) Majorana mass contribution M and a contribution induced by the electroweak-singlet A_4 -triplet Higgs boson χ when the A_4 -symmetry is spontaneously broken.

After the breaking of the flavor and electroweak symmetries, with the VEV alignments as in Eq. (15), the charged lepton, Dirac neutrino and right-handed neutrino mass terms from the Lagrangian (14) result in

$$-\mathcal{L}_{mW} = \frac{1}{2} \bar{N}_R^c M_R N_R + \bar{\nu}_L m_D N_R + \bar{\ell}_L m_\ell \ell_R + \frac{g}{\sqrt{2}} W_\mu^- \bar{\ell}_L \gamma^\mu \nu_L + \text{H.c.} \quad (34)$$

$$= \frac{1}{2} (\bar{\nu}_L \quad \bar{N}_R^c) \begin{pmatrix} 0 & m_D \\ m_D^T & M_R \end{pmatrix} \begin{pmatrix} \nu_L^c \\ N_R \end{pmatrix} + \bar{\ell}_L m_\ell \ell_R + \frac{g}{\sqrt{2}} W_\mu^- \bar{\ell}_L \gamma^\mu \nu_L + \text{H.c.} \quad (35)$$

Here $\ell = (e, \mu, \tau)$, $\nu = (\nu_e, \nu_\mu, \nu_\tau)$, $N_R = (N_{R1}, N_{R2}, N_{R3})$, and

$$m_\ell = \frac{v_\Phi}{\sqrt{2}} \begin{pmatrix} y_e & 0 & 0 \\ 0 & y_\mu & 0 \\ 0 & 0 & y_\tau \end{pmatrix}, \quad (36)$$

$$m_D = \frac{v_\eta}{\sqrt{2}} Y_\nu = \frac{v_\eta}{\sqrt{2}} \begin{pmatrix} y'_1 & y'_1 & y'_1 \\ y'_2 & \omega y'_2 & \omega^2 y'_2 \\ y'_3 & \omega^2 y'_3 & \omega y'_3 \end{pmatrix}, \quad (37)$$

$$M_R = \begin{pmatrix} M & 0 & 0 \\ 0 & M & y'_R v_\chi \\ 0 & y'_R v_\chi & M \end{pmatrix}. \quad (38)$$

To find the neutrino masses and mixing matrix we are to diagonalize the 6×6 matrix

$$\begin{pmatrix} 0 & m_D \\ m_D^T & M_R \end{pmatrix}. \quad (39)$$

We start by diagonalizing M_R . For this purpose, we perform a basis rotation $\hat{N}_R = U_R^\dagger N_R$, so that the right-handed Majorana mass matrix M_R becomes a diagonal matrix \hat{M}_R with real and positive mass eigenvalues $M_1 = aM$, $M_2 = M$ and $M_3 = bM$,

$$\begin{aligned} \hat{M}_R &= U_R^T M_R U_R = M U_R^T \begin{pmatrix} 1 & 0 & 0 \\ 0 & 1 & \kappa e^{i\xi} \\ 0 & \kappa e^{i\xi} & 1 \end{pmatrix} U_R \\ &= \begin{pmatrix} aM & 0 & 0 \\ 0 & M & 0 \\ 0 & 0 & bM \end{pmatrix}, \end{aligned} \quad (40)$$

where $\kappa = |y'_R v_\chi / M|$ and $\xi = \arg(y'_R v_\chi / M)$. We find $a = \sqrt{1 + \kappa^2 + 2\kappa \cos \xi}$, $b = \sqrt{1 + \kappa^2 - 2\kappa \cos \xi}$, and a diagonalizing matrix

$$U_R = \frac{1}{\sqrt{2}} \begin{pmatrix} 0 & \sqrt{2} & 0 \\ 1 & 0 & -1 \\ 1 & 0 & 1 \end{pmatrix} \begin{pmatrix} e^{i\frac{\phi_1}{2}} & 0 & 0 \\ 0 & 1 & 0 \\ 0 & 0 & e^{i\frac{\phi_2}{2}} \end{pmatrix}, \quad (41)$$

with phases

$$U_{\text{PMNS}} = \begin{pmatrix} c_{13}c_{12} & c_{13}s_{12} & s_{13}e^{-i\delta_{CP}} \\ -c_{23}s_{12} - s_{23}c_{12}s_{13}e^{i\delta_{CP}} & c_{23}c_{12} - s_{23}s_{12}s_{13}e^{i\delta_{CP}} & s_{23}c_{13} \\ s_{23}s_{12} - c_{23}c_{12}s_{13}e^{i\delta_{CP}} & -s_{23}c_{12} - c_{23}s_{12}s_{13}e^{i\delta_{CP}} & c_{23}c_{13} \end{pmatrix} Q_\nu, \quad (49)$$

where $Q_\nu = \text{Diag}(e^{-i\phi_1/2}, e^{-i\phi_2/2}, 1)$, and $s_{ij} \equiv \sin\theta_{ij}$ and $c_{ij} \equiv \cos\theta_{ij}$.

It is important to notice that the phase matrix P_ν can be rotated away by choosing the matrix $P_\ell = P_\nu$, i.e., by an appropriate redefinition of the left-handed

$$\begin{aligned} \psi_1 &= \tan^{-1} \left(\frac{-\kappa \sin \xi}{1 + \kappa \cos \xi} \right) \quad \text{and} \\ \psi_2 &= \tan^{-1} \left(\frac{\kappa \sin \xi}{1 - \kappa \cos \xi} \right). \end{aligned} \quad (42)$$

As the magnitude of κ defined in Eq. (40) decreases, the phases $\psi_{1,2}$ go to 0 or π . At this point,

$$\begin{aligned} -\mathcal{L}_{mW} &= \frac{1}{2} \begin{pmatrix} \bar{\nu}_L & \tilde{N}_R^c \end{pmatrix} \begin{pmatrix} 0 & \tilde{m}_D \\ \tilde{m}_D^T & \hat{M}_R \end{pmatrix} \begin{pmatrix} \nu_L^c \\ \hat{N}_R \end{pmatrix} + \bar{\ell}_L m_\ell \ell_R \\ &+ \frac{g}{\sqrt{2}} W_\mu^- \bar{\ell}_L \gamma^\mu \nu_L + \text{H.c.}, \end{aligned} \quad (43)$$

with $\tilde{m}_D = m_D U_R$.

Now we take the limit of large M (seesaw mechanism) and focus on the mass matrix of the light neutrinos M_ν ,

$$\begin{aligned} -\mathcal{L}_{mW} &= \frac{1}{2} \bar{\nu}_L M_\nu \nu_L^c + \bar{\ell}_L m_\ell \ell_R + \frac{g}{\sqrt{2}} W_\mu^- \bar{\ell}_L \gamma^\mu \nu_L \\ &+ \text{H.c.} + \text{terms in } N_R, \end{aligned} \quad (44)$$

with

$$M_\nu = -\tilde{m}_D \hat{M}_R^{-1} \tilde{m}_D^T. \quad (45)$$

We perform basis rotations from weak to mass eigenstates in the leptonic sector,

$$\hat{\ell}_L = P_\ell^* \ell_L, \quad \hat{\ell}_R = P_\ell^* \ell_R, \quad \hat{\nu}_L = U_\nu^\dagger P_\nu^* \nu_L, \quad (46)$$

where P_ℓ and P_ν are phase matrices and U_ν is a unitary matrix chosen so as the matrix

$$\begin{aligned} \hat{m}_\nu &= U_\nu^\dagger P_\nu^* M_\nu P_\nu^* U_\nu \\ &= -U_\nu^\dagger P_\nu^* m_D U_R \hat{M}_R^{-1} (U_\nu^\dagger P_\nu^* m_D U_R)^T \end{aligned} \quad (47)$$

is diagonal. Then from the charged current term in Eq. (43) we obtain the lepton mixing matrix U_{PMNS} as

$$U_{\text{PMNS}} = P_\ell^* P_\nu U_\nu. \quad (48)$$

The matrix U_{PMNS} can be written in terms of three mixing angles and three CP -odd phases (one for the Dirac neutrinos and two for the Majorana neutrinos) as [1]

charged lepton fields, which is always possible. This is an important point because the phase matrix P_ν accompanies the Dirac-neutrino mass matrix \tilde{m}_D and ultimately the neutrino Yukawa matrix Y_ν in Eq. (37). This means that complex phases in Y_ν can always be

rotated away by appropriately choosing the phases of left-handed charged lepton fields. Hence without loss of generality the eigenvalues y_1^ν , y_2^ν , and y_3^ν of Y_ν can be real and positive. The Yukawa matrix Y_ν can then be written as

$$Y_\nu = y_3^\nu \sqrt{3} \begin{pmatrix} y_1 & 0 & 0 \\ 0 & y_2 & 0 \\ 0 & 0 & 1 \end{pmatrix} U_\omega^\dagger, \quad (50)$$

where $y_1 = |y_1^\nu/y_3^\nu|$, $y_2 = |y_2^\nu/y_3^\nu|$, and U_ω is given in Eq. (9).

Concerning CP violation, we notice that the CP phases ψ_1, ψ_2 coming from M_R only take part in low-energy CP violation, as can be seen in Eqs. (40)–(50). Any CP -violation relevant for leptogenesis is associated with the neutrino Yukawa matrix $\tilde{Y}_\nu = Y_\nu U_R$ and the combination of Dirac neutrino Yukawa matrices, $H \equiv \tilde{Y}_\nu^\dagger \tilde{Y}_\nu = U_R^\dagger Y_\nu^\dagger Y_\nu U_R$, which is

$$H = 3|y_3^\nu|^2 \begin{pmatrix} \frac{1+4y_1^2+y_2^2}{2} & \frac{e^{-i\frac{\psi_1}{2}}}{\sqrt{2}}(2y_1^2 - y_2^2 - 1) & \frac{i\sqrt{3}e^{i\frac{\psi_{21}}{2}}}{2}(y_2^2 - 1) \\ \frac{e^{i\frac{\psi_1}{2}}}{\sqrt{2}}(2y_1^2 - y_2^2 - 1) & 1 + y_1^2 + y_2^2 & -i\sqrt{\frac{3}{2}}e^{i\frac{\psi_2}{2}}(y_2^2 - 1) \\ -\frac{i\sqrt{3}e^{-i\frac{\psi_{21}}{2}}}{2}(y_2^2 - 1) & i\sqrt{\frac{3}{2}}e^{-i\frac{\psi_2}{2}}(y_2^2 - 1) & \frac{3}{2}(1 + y_2^2) \end{pmatrix}, \quad (51)$$

where $\psi_{ij} \equiv \psi_i - \psi_j$. As expected, in the limit $|y_1^\nu| = |y_2^\nu| = |y_3^\nu|$, i.e., $y_{1,2} \rightarrow 1$, the off-diagonal entries of H vanish, and there is no CP violation useful for leptogenesis. If the Dirac neutrino Yukawa couplings y_1^ν, y_2^ν , and y_3^ν differ in magnitude, they can play a role in baryogenesis via leptogenesis and nonzero $\theta_{13} \simeq 9^\circ$ with TBM ($\theta_{23} \simeq 45^\circ, \theta_{12} \simeq 35^\circ$). Therefore, a low-energy CP violation in neutrino oscillation and/or a high-energy CP violation in leptogenesis can be generated by the nondegeneracy of the Dirac neutrino Yukawa couplings and a nonzero phase ξ coming from M_R .

In the following section we investigate the low-energy phenomenology, namely the possible values of the light neutrino mixing angles, how the low-energy CP violation could be generated in both normal and inverted mass hierarchies, and neutrinoless double beta decay, which is a probe of lepton number violation at low energy.

III. PHENOMENOLOGY OF LIGHT NEUTRINOS

After seesawing, in a basis where charged lepton and heavy neutrino masses are real and diagonal, the light neutrino mass matrix is given by

$$m_\nu = -\tilde{m}_D \hat{M}_R^{-1} \tilde{m}_D^T = -\frac{\mathbf{v}_\eta^2}{2} Y_\nu U_R \hat{M}_R^{-1} U_R^T Y_\nu^T = m_0 \begin{pmatrix} \left(1 + \frac{2e^{i\psi_1}}{a}\right)y_1^2 & \left(1 - \frac{e^{i\psi_1}}{a}\right)y_1 y_2 & \left(1 - \frac{e^{i\psi_1}}{a}\right)y_1 \\ \left(1 - \frac{e^{i\psi_1}}{a}\right)y_1 y_2 & \left(1 + \frac{e^{i\psi_1}}{2a} - \frac{3e^{i\psi_2}}{2b}\right)y_2^2 & \left(1 + \frac{e^{i\psi_1}}{2a} + \frac{3e^{i\psi_2}}{2b}\right)y_2 \\ \left(1 - \frac{e^{i\psi_1}}{a}\right)y_1 & \left(1 + \frac{e^{i\psi_1}}{2a} + \frac{3e^{i\psi_2}}{2b}\right)y_2 & \left(1 + \frac{e^{i\psi_1}}{2a} - \frac{3e^{i\psi_2}}{2b}\right) \end{pmatrix}, \quad (52)$$

where $\tilde{m}_D = \mathbf{v}_\eta \tilde{Y}_\nu / \sqrt{2}$ and we have defined an overall scale $m_0 = \mathbf{v}_\eta^2 |y_3^\nu|^2 / (6M)$ for the light neutrino masses. The mass matrix m_ν is diagonalized by the PMNS mixing matrix U_{PMNS} as described above,

$$m_\nu = U_{\text{PMNS}} \text{Diag}(m_1, m_2, m_3) U_{\text{PMNS}}^T. \quad (53)$$

Here m_i ($i = 1, 2, 3$) are the light neutrino masses. As is well known, because of the observed hierarchy $|\Delta m_{\text{Atm}}^2| \equiv |m_3^2 - m_1^2| \gg \Delta m_{\text{sol}}^2 \equiv m_2^2 - m_1^2 > 0$, and the requirement of a Mikheyev-Smirnov-Wolfenstein resonance for solar neutrinos, there are two possible neutrino mass spectra: (i) the normal mass hierarchy (NMH) $m_1 < m_2 < m_3$, and (ii) the inverted mass hierarchy (IMH) $m_3 < m_1 < m_2$.

Interestingly, the combination $U_\omega^\dagger U_R$ in Eq. (52) reflects an exact TBM:

$$U_\omega^\dagger U_R = \begin{pmatrix} \sqrt{\frac{2}{3}} & \frac{1}{\sqrt{3}} & 0 \\ -\frac{1}{\sqrt{6}} & \frac{1}{\sqrt{3}} & -\frac{1}{\sqrt{2}} \\ -\frac{1}{\sqrt{6}} & \frac{1}{\sqrt{3}} & \frac{1}{\sqrt{2}} \end{pmatrix} \begin{pmatrix} e^{i\frac{\psi_1}{2}} & 0 & 0 \\ 0 & 1 & 0 \\ 0 & 0 & e^{i\frac{\psi_2}{2} + \pi} \end{pmatrix}. \quad (54)$$

Therefore Eq. (52) directly indicates that there could be deviations from the exact TBM if the Dirac neutrino Yukawa couplings do not have the same magnitude. In the limit $|y_2^\nu| = |y_3^\nu|$ ($y_2 \rightarrow 1$), the mass matrix in Eq. (52) acquires a μ - τ symmetry that leads to $\theta_{13} = 0$ and $\theta_{23} = -\pi/4$. Moreover, in the limit $|y_1^\nu| = |y_2^\nu| = |y_3^\nu|$ ($y_1, y_2 \rightarrow 1$), the mass matrix (52) gives the TBM angles in Eq. (1) and the corresponding mass eigenvalues

$$m_1 = \frac{3m_0}{a}, \quad m_2 = 3m_0, \quad m_3 = \frac{3m_0}{b}. \quad (55)$$

These mass eigenvalues are disconnected from the mixing angles. However, recent neutrino data, i.e., $\theta_{13} \neq 0$,

require deviations of $y_{1,2}$ from unity, leading to a possibility to search for CP violation in neutrino oscillation experiments. These deviations generate relations between mixing angles and mass eigenvalues.

To diagonalize the above mass matrix Eq. (52), we consider the Hermitian matrix $m_\nu m_\nu^\dagger = U_{\text{PMNS}} \text{Diag}(m_1^2, m_2^2, m_3^2) \times U_{\text{PMNS}}^\dagger$, from which we obtain the masses and mixing angles. To see how the neutrino mass matrix given by Eq. (52) can lead to deviations of neutrino mixing angles from their TBM values, we first introduce three small quantities

ϵ_i , ($i = 1, 2, 3$), which are responsible for the deviations of the θ_{jk} from their TBM values:

$$\begin{aligned}\theta_{23} &= -\frac{\pi}{4} + \epsilon_1, & \theta_{13} &= \epsilon_2, \\ \theta_{12} &= \sin^{-1}\left(\frac{1}{\sqrt{3}}\right) + \epsilon_3.\end{aligned}\quad (56)$$

Then the PMNS mixing matrix up to order ϵ_i can be written as

$$U_{\text{PMNS}} = \begin{pmatrix} \frac{\sqrt{2}-\epsilon_3}{\sqrt{3}} & \frac{1+\epsilon_3\sqrt{2}}{\sqrt{3}} & \epsilon_2 e^{-i\delta_{CP}} \\ -\frac{1+\epsilon_1+\epsilon_3\sqrt{2}}{\sqrt{6}} + \frac{\epsilon_2 e^{i\delta_{CP}}}{\sqrt{3}} & \frac{\sqrt{2}+\epsilon_1\sqrt{2}-\epsilon_3}{\sqrt{6}} + \frac{\epsilon_2 e^{i\delta_{CP}}}{\sqrt{6}} & \frac{-1+\epsilon_1}{\sqrt{2}} \\ \frac{-1+\epsilon_1+\epsilon_3\sqrt{2}}{\sqrt{6}} - \frac{\epsilon_2 e^{i\delta_{CP}}}{\sqrt{3}} & \frac{\sqrt{2}-\epsilon_3-\sqrt{2}\epsilon_1}{\sqrt{6}} - \frac{\epsilon_2 e^{i\delta_{CP}}}{\sqrt{6}} & \frac{1+\epsilon_1}{\sqrt{2}} \end{pmatrix} Q_\nu + \mathcal{O}(\epsilon_i^2). \quad (57)$$

The small deviation ϵ_1 from the maximality of the atmospheric mixing angle θ_{23} is expressed in terms of the parameters in Eq. (B1) in Appendix B as

$$\tan\epsilon_1 = \frac{R(1+y_2) - S(y_2-1)}{R(y_2-1) - S(1+y_2)}. \quad (58)$$

In the limit of $y_1, y_2 \rightarrow 1$, ϵ_1 goes to zero (or equivalently $\theta_{23} \rightarrow -\pi/4$) due to $R, S \rightarrow 0$. The reactor angle θ_{13} and the Dirac- CP phase δ_{CP} are expressed as

$$\begin{aligned}\tan 2\theta_{13} &= \frac{y_1 |s_{23}(3Q-P)y_2 - c_{23}(3Q+P) - 3i\{s_{23}(R-S)y_2 + c_{23}(R+S)\}|}{(F+G+\frac{9K}{4}+\frac{3D}{2})(c_{23}^2+y_2^2s_{23}^2) + y_2(F+G-\frac{9K}{4})\sin 2\theta_{23} - y_1^2\tilde{A}}, \\ \tan\delta_{CP} &= 3\frac{(R-S)^2 + y_2^2(R+S)^2}{(P+Q)(R-S) - y_2^2(P-Q)(R+S)},\end{aligned}\quad (59)$$

where the parameters P, Q, F, G, K, D and \tilde{A} are given in Eq. (B1) in Appendix B. In the limit of $y_1, y_2 \rightarrow 1$, the parameters Q, R, S go to zero, which in turn leads to $\theta_{13} \rightarrow 0$ and $\delta_{CP} \rightarrow 0$ as expected. Finally, the solar mixing angle is given by

$$\tan 2\theta_{12} = 2y_1 \frac{y_2 c_{23}(3Q-P) + s_{23}(3Q+P)}{c_{13}(\Psi_2 - \Psi_1)}. \quad (60)$$

Since in the limit $y_1, y_2 \rightarrow 1$ the parameters in Eq. (60) behave as $Q \rightarrow 0$, $P \rightarrow 6(\frac{1}{a^2} - 1)$, $\Psi_1 \rightarrow 3(1 + \frac{2}{a^2})$ and $\Psi_2 \rightarrow 6(1 + \frac{1}{2a^2})$, it is clear that the mixing angle $\tan 2\theta_{12}$ goes to $2\sqrt{2}$, that is, $\theta_{12} \rightarrow \sin^{-1}(1/\sqrt{3})$.

The squared-mass eigenvalues of the three light neutrinos result in

$$\begin{aligned}m_1^2 &= m_0^2 \left\{ s_{12}^2 \Psi_1 + c_{12}^2 \Psi_2 - y_1 \frac{y_2 c_{23}(3Q-P) + s_{23}(3Q+P)}{2c_{13}} \sin 2\theta_{12} \right\}, \\ m_2^2 &= m_0^2 \left\{ c_{12}^2 \Psi_1 + s_{12}^2 \Psi_2 + y_1 \frac{y_2 c_{23}(3Q-P) + s_{23}(3Q+P)}{2c_{13}} \sin 2\theta_{12} \right\}, \\ m_3^2 &= m_0^2 \left\{ \left[(F+G+\frac{9K}{4}+\frac{3D}{2})(c_{23}^2+y_2^2s_{23}^2) + y_2(F+G-\frac{9K}{4})\sin 2\theta_{23} \right] c_{13}^2 + y_1^2 \tilde{A} s_{13}^2 \right. \\ &\quad \left. - \frac{y_1 \sin 2\theta_{13}}{2} [c_{23}((3Q+P)\cos\delta_{CP} - 3(R+S)\sin\delta_{CP}) + s_{23}y_2((3Q-P)\cos\delta_{CP} + 3(R-S)\sin\delta_{CP})] \right\}.\end{aligned}\quad (61)$$

We see from Eqs. (60) and (61) that the deviation ϵ_3 from tri-maximality of solar mixing angle θ_{12} can be expressed as

$$2\sqrt{2}\cos 2\epsilon_3 + \sin 2\epsilon_3 = \frac{3y_1 m_0^2 \{y_2 c_{23}(3Q-P) + s_{23}(3Q+P)\}}{c_{13} \Delta m_{21}^2}. \quad (62)$$

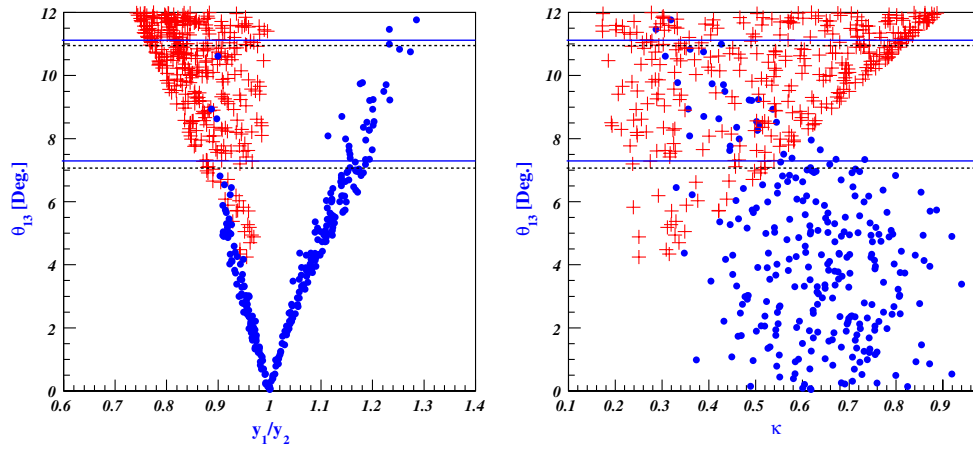


FIG. 1 (color online). The reactor mixing angle θ_{13} versus the ratio of first-to-second generation neutrino Yukawa couplings y_1^ν/y_2^ν (left-hand plot) and the parameter $\kappa = |y_k^\nu v_\chi/M|$ (right-hand plot). The (red) crosses and (blue) dots represent the results for the normal and the inverted mass hierarchy, respectively. The horizontal solid (dotted) lines in both plots indicate the upper and lower bounds on θ_{13} for inverted (normal) mass hierarchy given in Eq. (64) at the 3σ level.

Now we perform a numerical analysis using the linear algebra tools in Ref. [20]. The Daya Bay and RENO experiments have accomplished the measurement of three mixing angles θ_{12} , θ_{23} , and θ_{13} from three kinds of neutrino oscillation experiments. A combined analysis of the data from the T2K, MINOS, Double Chooz, Daya Bay and RENO experiments shows [7] that, for the normal mass hierarchy (NMH) and inverted mass hierarchy (IMH), respectively,

$$\sin^2\theta_{13} = 0.026_{-0.004(-0.011)}^{+0.003(+0.010)} \text{NMH},$$

$$\left[0.027_{-0.004(-0.011)}^{+0.003(+0.010)}\right] \text{IMH} \quad (63)$$

or equivalently

$$\theta_{13} = 9.28_{-0.75(-2.24)}^{+0.53(+1.66)} \text{NMH},$$

$$\left[9.46_{-0.73(-2.19)}^{+0.52(+1.64)}\right] \text{IMH} \quad (64)$$

at the 1σ (3σ) level. The hypothesis $\theta_{13} = 0$ is now rejected at the 8σ significance level. In addition to the measurement of the mixing angle θ_{13} , the global fit of the neutrino mixing angles and of the mass-squared differences at the 1σ (3σ) level is given by [7]

$$\theta_{12} = 34.45_{-1.05(-3.14)}^{+0.92(+3.02)},$$

$$\theta_{23} = 44.43_{-2.87(-5.78)}^{+4.60(+8.70)} \text{NMH},$$

$$\left[46.72_{-4.01(-8.07)}^{+2.89(+6.41)}\right] \text{IMH}$$

$$\Delta m_{\text{Sol}}^2 [10^{-5} \text{ eV}^2] = 7.62_{-0.19(-0.50)}^{+0.19(+0.58)},$$

$$\Delta m_{\text{Atm}}^2 [10^{-3} \text{ eV}^2] = \begin{cases} 2.53_{-0.10(-0.27)}^{+0.08(+0.24)} & \text{NMH} \\ 2.40_{-0.07(-0.25)}^{+0.10(+0.28)} & \text{IMH} \end{cases} \quad (65)$$

The matrices m_D and \hat{M}_R in Eq. (52) contain seven parameters : y_3^ν , M , v_η , y_1 , y_2 , κ , ξ . The first three

(y_3^ν , M , and v_η) lead to the overall neutrino scale parameter m_0 . The next four (y_1 , y_2 , κ , ξ) give rise to the deviations from TBM as well as the CP phases and corrections to the mass eigenvalues [see Eq. (55)].

In our numerical examples, we take $M = 10$ TeV and $v_\eta = v_\Phi = 123$ GeV, for simplicity, as inputs. Since the neutrino masses are sensitive to the combination $m_0 = v_\eta^2 |y_3^\nu|^2 / (6M)$, other choices of M and v_η give identical results. Then the parameters m_0 , y_1 , y_2 , κ , ξ can be determined from the experimental results of three mixing angles, θ_{12} , θ_{13} , θ_{23} , and the two mass-squared differences, Δm_{21}^2 , Δm_{31}^2 . In addition, the CP phases δ_{CP} , $\varphi_{1,2}$ can be predicted after determining the model parameters. Using the formulas for the neutrino mixing angles and masses and our values of M , v_η , v_Φ , we obtain the following allowed regions of the unknown model parameters: for the normal mass hierarchy (NMH),⁴

$$0.17 \lesssim \kappa \lesssim 0.90, \quad 0.74 \lesssim y_1 \lesssim 1.0,$$

$$0.90 \lesssim y_2 \lesssim 1.11, \quad 94^\circ \lesssim \xi \lesssim 119^\circ$$

$$240^\circ \lesssim \xi \lesssim 265^\circ, \quad 1.8 \lesssim m_0 \times 10^{-2} [\text{eV}] \lesssim 6.0; \quad (66)$$

For the inverted mass hierarchy (IMH),

$$0.31 \lesssim \kappa \lesssim 0.92, \quad 0.84 \lesssim y_1 \lesssim 1.15,$$

$$0.65 \lesssim y_2 \lesssim 1.28, \quad 90^\circ \lesssim \xi \lesssim 117^\circ$$

$$245^\circ \lesssim \xi \lesssim 265^\circ, \quad 1.7 \lesssim m_0 \times 10^{-2} [\text{eV}] \lesssim 4.5. \quad (67)$$

Note that here we have used the 3σ experimental bounds on θ_{12} , θ_{23} , Δm_{21}^2 , Δm_{31}^2 in Eq. (65), except for $\theta_{13} < 12^\circ$ for which we use the values in Eqs. (66) and (67). For these

⁴When $y_2 = 1$ and around there, there exist other parameter spaces giving very small values of θ_{13} . So, we have neglected them in our numerical result for normal mass hierarchy.

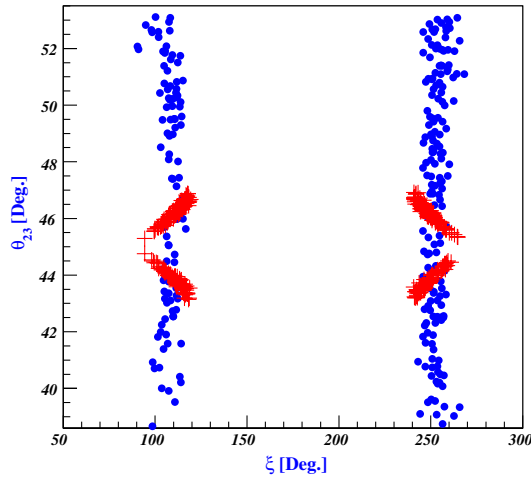


FIG. 2 (color online). The atmospheric mixing angle θ_{23} versus the phase ξ of the parameter combination $y_R^{\nu} v_{\chi}/M$. The (red) crosses and (blue) dots represent the results for the normal and inverted mass hierarchy, respectively.

parameter regions, we investigate how a nonzero θ_{13} can be determined for the normal and inverted mass hierarchy. In Figs. 1–5, the data points represented by (blue) dots and (red) crosses indicate results for the inverted and normal mass hierarchy, respectively. The left-hand plot in Fig. 1 shows how the mixing angle θ_{13} depends on the ratio $y_1/y_2 = y_1^{\nu}/y_2^{\nu}$ of the first- and second-generation neutrino Yukawa couplings; the right-hand plot shows how θ_{13} depends on the parameter $\kappa = |y_R^{\nu} v_{\chi}/M|$. We see that the measured value of θ_{13} from the Daya Bay and RENO experiments can be achieved at 3σ 's for $0.75 < y_1/y_2 < 1$ (NMH), $1.1 < y_1/y_2 < 1.3$ and $y_1/y_2 \sim 0.9$ (IMH), $0.17 \lesssim \kappa \lesssim 0.82$ (NMH) and $0.3 < \kappa \lesssim 0.74$ (IMH). Figure 2 shows the atmospheric mixing angle θ_{23} as a function of the phase ξ of $y_R^{\nu} v_{\chi}/M$.

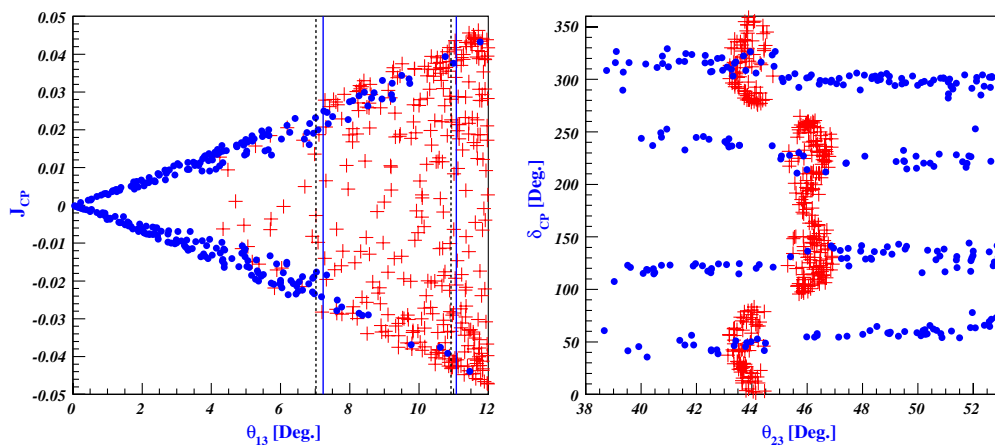


FIG. 3 (color online). The Jarlskog invariant J_{CP} versus the reactor angle θ_{13} (left-hand plot), and the Dirac CP phase δ_{CP} versus θ_{23} (right-hand plot). The (red) crosses and (blue) dots represent the results for the normal and inverted mass hierarchy, respectively. The vertical solid (dashed) lines in both plots indicate the upper and lower bounds on θ_{13} for the inverted (normal) mass hierarchy given in Eq. (64) at the 3σ level.

To see how the parameters are correlated with low-energy CP violation observables measurable through neutrino oscillations, we consider the leptonic CP violation parameter defined by the Jarlskog invariant [21]

$$\begin{aligned} J_{CP} &\equiv \text{Im}[U_{e1}U_{\mu 2}U_{e2}^*U_{\mu 1}^*] \\ &= \frac{1}{8} \sin 2\theta_{12} \sin 2\theta_{23} \sin 2\theta_{13} \cos \theta_{13} \sin \delta_{CP}. \end{aligned} \quad (68)$$

The Jarlskog invariant J_{CP} can be expressed in terms of the elements of the matrix $h = m_{\nu} m_{\nu}^{\dagger}$ [22]:

$$J_{CP} = -\frac{\text{Im}\{h_{12}h_{23}h_{31}\}}{\Delta m_{21}^2 \Delta m_{31}^2 \Delta m_{32}^2}. \quad (69)$$

The behavior of J_{CP} as a function of θ_{13} is plotted on the left-hand plot of Fig. 3. We see that the value of $|J_{CP}|$ lies in the range 0–0.04 (NMH) and 0.02–0.04 (IMH) for the measured value of θ_{13} at 3σ 's. Also, in our model we have

$$\text{Im}\{h_{12}h_{23}h_{31}\} = \frac{27m_0^6}{4a^4b^3} y_1^2 y_2^2 (1 - y_2^2) \sin \psi_2 \{\dots\}, \quad (70)$$

in which $\{\dots\}$ stands for a complicated lengthy function of y_1, y_2, a, b, ψ_1 and ψ_2 . Clearly, Eq. (70) indicates that in the limit of $y_2 \rightarrow 1$ or $\sin \psi_2 \rightarrow 0$ the leptonic CP violation J_{CP} goes to zero. When $y_2 \neq 1$, i.e., for the normal hierarchy case, J_{CP} could go to zero as $\sin \psi_2$ of Eq. (70). In the case of the inverted hierarchy, J_{CP} has nonzero values for the measured range of θ_{13} while J_{CP} goes to zero for $\theta_{13} \rightarrow 0$, which corresponds to $y_2 \rightarrow 1$. The right-hand plot of Fig. 3 shows the behavior of the Dirac CP phase δ_{CP} as a function of θ_{23} , where δ_{CP} can have discrete values around $50^\circ, 120^\circ, 230^\circ$, and 310° for the inverted mass hierarchy (for the normal mass hierarchy, δ_{CP} can vary over a wide range except near 90° and 270°). Future precise measurements of θ_{23} , whether $\theta_{23} > 45^\circ$ or $\theta_{23} < 45^\circ$, will provide more information on δ_{CP} .

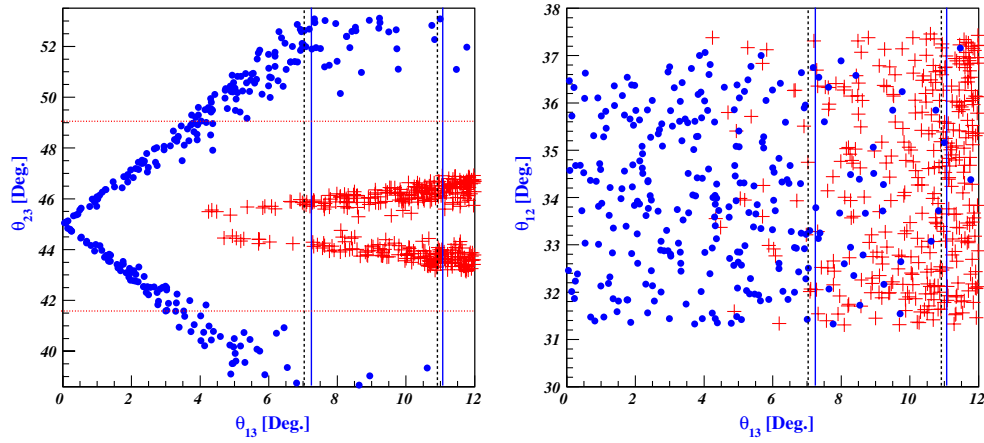


FIG. 4 (color online). The behaviors of θ_{23} and θ_{12} in terms of θ_{13} . The (red) crosses and the (blue) dots represent results for the normal mass hierarchy and the inverted mass hierarchy, respectively. The solid (dashed) vertical lines represent the experimental bounds of Eq. (65) at 3σ 's for the inverted (normal) mass hierarchy. The horizontal dotted lines indicate the 1σ experimental bounds in Eq. (65).

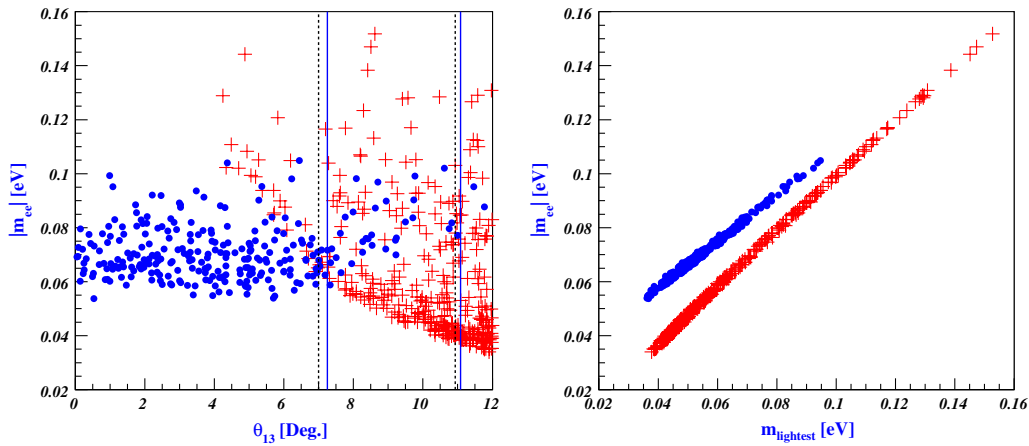


FIG. 5 (color online). Plots of $|m_{ee}|$ as a function of θ_{13} and m_{lightest} . The (red) crosses and the (blue) dots represent results for the normal and the inverted mass hierarchy, respectively. The vertical solid (dashed) lines show the experimental bounds of Eq. (65) at 3σ 's for the inverted (normal) mass hierarchy.

Figure 4 shows how the values of θ_{13} depend on the mixing angles θ_{23} and θ_{12} . As can be seen in the left-hand plot of Fig. 4, the behavior of θ_{23} in terms of the measured values of θ_{13} at 3σ 's for the normal hierarchy is different than for the inverted hierarchy. For the normal hierarchy we see that the measured values of θ_{13} can be achieved for $43^\circ < \theta_{23} < 47^\circ$ and $\theta_{23} \neq 45^\circ$, with small deviations from maximality, while for the inverted hierarchy $50^\circ \leq \theta_{23} \leq 53.1^\circ$ and $38.6^\circ \leq \theta_{23} \leq 40^\circ$, which are excluded at 1σ by the experimental bounds as can be seen in Eq. (65).⁵ From the right-hand plot of Fig. 4, we see that the predictions for θ_{13} do not strongly depend on θ_{12} in the allowed region.

⁵Interestingly, the most recent data of MINOS seem to disfavor the maximal mixing in the atmospheric mixing angle, Eq. (4), indicating that the inverted mass hierarchy may be favored.

Moreover, we can straightforwardly obtain the effective neutrino mass $|m_{ee}|$ that characterizes the amplitude for neutrinoless double beta decay:

$$|m_{ee}| \equiv \left| \sum_i (U_{\text{PMNS}})_{ei}^2 m_i \right|, \quad (71)$$

where U_{PMNS} is given in Eq. (57). The left-hand and right-hand plots in Fig. 5 show the behavior of the effective neutrino mass $|m_{ee}|$ in terms of θ_{13} and the lightest neutrino mass, respectively. In the left-hand plot of Fig. 5, for the measured values of θ_{13} at 3σ 's, the effective neutrino mass $|m_{ee}|$ can be in the range $0.04 \leq |m_{ee}|[\text{eV}] < 0.15$ (NMH) or $0.06 \leq |m_{ee}|[\text{eV}] \leq 0.11$ (IMH). The right-hand plot of Fig. 5 shows $|m_{ee}|$ as a function of m_{lightest} , where $m_{\text{lightest}} = m_1$ for the normal mass hierarchy and $m_{\text{lightest}} = m_3$ for the inverted mass hierarchy. Our model predicts that the effective mass

$|m_{ee}|$ is within the sensitivity of planned neutrinoless double-beta decay experiments.

IV. CONCLUSIONS

We have suggested a novel and simple scenario to generate neutrino masses and mixings with a discrete A_4 symmetry that is spontaneously broken. In particular our model can accommodate in a renormalizable Lagrangian a large value of the mixing angle, θ_{13} , consistent with the recent reactor neutrino experiments Daya Bay and RENO, as well as high-energy CP violation interesting for leptogenesis.

In our model we have introduced a right-handed neutrino N_R , a real gauge-singlet scalar χ , and an $SU(2)_L$ -doublet scalar η , all of which are A_4 triplets. The light neutrino masses are generated by a seesaw mechanism in which we have assumed the right-handed neutrino masses are at the TeV scale (to evade the introduction of higher-dimensional operators). Getting VEVs along the direction $\langle \chi \rangle = v_\chi(1, 0, 0)$ and $\langle \eta^0 \rangle = v_\eta(1, 1, 1)$, which break the A_4 symmetry down to a Z_2 (S -flavor-parity) and a Z_3 (T -flavor) symmetry, respectively, one obtains bimaximal mixing at the right-handed neutrino sector and trimaximal mixing at the light Dirac neutrino sector with nondegenerate Yukawa couplings that deform the exact TBM pattern. The resulting light neutrino mixing matrix is in the form of a deviated TBM generated through unequal neutrino Yukawa couplings, as can be seen in Fig. 1. In the limiting case of equal active-neutrino Yukawa couplings, the mixing matrix recovers the exact TBM. In addition, we have shown that unequal neutrino Yukawa couplings can provide a source of high-energy CP violation, perhaps strong enough to be responsible for leptogenesis. The stability of the vacuum alignments we assume are guaranteed, for example, by embedding our model in an extra dimension.

We showed that deviations from the TBM of about 20% are enough to explain $\theta_{13} \sim 9^\circ$. We predicted that the CP violating Dirac phase δ_{CP} may have discrete values (see Fig. 3). Therefore the measurement of the phase δ_{CP} in the next-generation neutrino experiments can rule out or support our model. We have also shown that the inverted mass hierarchy may be excluded by a global analysis using 1σ experimental bounds, while the most recent MINOS data seem to favor it. We also predicted an effective neutrino mass in neutrinoless double-beta decay in the range, $0.04 \leq |m_{ee}|[\text{eV}] < 0.15$ (for the normal hierarchy) and $0.06 \leq |m_{ee}|[\text{eV}] \leq 0.11$ (for the inverted hierarchy), both ranges within reach of near-future neutrinoless double beta decay experiments.

ACKNOWLEDGMENTS

This work was supported by NRF Research Grant No. 2012R1A2A1A01006053 (SB). P.G. was supported in part by NSF Grant No. PHY-1068111 at the University of Utah and thanks the Korean Instituted for Advanced

Studies and Seoul National University for support during the completion of this work.

APPENDIX A: THE HIGGS POTENTIAL

In this appendix we present our Higgs potential and its minimization, as well as our prescription for effecting the stability of the vacuum alignment. We solve the vacuum alignment problem by extending the model into a spatial extra dimension y [12]. We assume that each field lives on a 4D brane either at $y = 0$ or at $y = L$, as shown in Fig. 6. The heavy neutrino masses arise from local operators at $y = 0$, while the charged fermion masses and the neutrino Yukawa interactions are realized by nonlocal effects involving both branes, a rigorous explanation of this possibility is beyond the scope of this paper.

The most general renormalizable scalar potential for the Higgs fields Φ , η and χ , invariant under $SU(2)_L \times U(1)_Y \times A_4$ and obeying the conditions in the previous paragraph, is then given by

$$V = V_{y=0} + V_{y=L}, \quad (\text{A1})$$

where

$$V_{y=0} = V(\Phi) + V(\eta) + V(\eta\Phi), \quad (\text{A2})$$

$$V_{y=L} = V(\chi), \quad (\text{A3})$$

and

$$\begin{aligned} V(\eta) = & \mu_\eta^2 (\eta^\dagger \eta)_1 + \lambda_1^\eta (\eta^\dagger \eta)_1 (\eta^\dagger \eta)_1 + \lambda_2^\eta (\eta^\dagger \eta)_{1'} (\eta^\dagger \eta)_{1''} \\ & + \lambda_3^\eta (\eta^\dagger \eta)_{3_s} (\eta^\dagger \eta)_{3_s} + \lambda_4^\eta (\eta^\dagger \eta)_{3_a} (\eta^\dagger \eta)_{3_a} \\ & + \{\lambda_5^\eta (\eta^\dagger \eta)_{3_s} (\eta^\dagger \eta)_{3_a} + \text{H.c.}\}, \end{aligned} \quad (\text{A4})$$

$$V(\Phi) = \mu_\Phi^2 (\Phi^\dagger \Phi) + \lambda^\Phi (\Phi^\dagger \Phi)^2,$$

$$\begin{aligned} V(\chi) = & \mu_\chi^2 (\chi\chi)_1 + \lambda_1^\chi (\chi\chi)_1 (\chi\chi)_1 + \lambda_2^\chi (\chi\chi)_{1'} (\chi\chi)_{1''} \\ & + \lambda_3^\chi (\chi\chi)_{3_s} (\chi\chi)_{3_s} + \lambda_4^\chi (\chi\chi)_{3_a} (\chi\chi)_{3_a} \\ & + \lambda_5^\chi (\chi\chi)_{3_s} (\chi\chi)_{3_a} + \xi_1^\chi \chi (\chi\chi)_{3_s} + \xi_2^\chi \chi (\chi\chi)_{3_a}, \end{aligned} \quad (\text{A5})$$

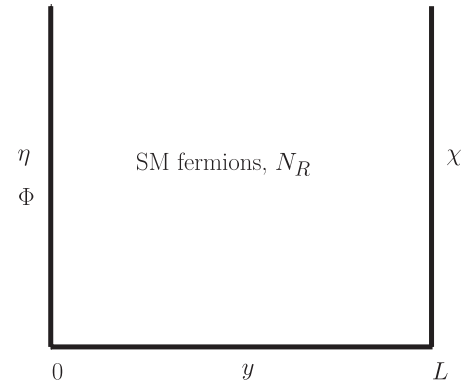


FIG. 6. Fifth dimension y and locations of scalar and fermion fields on the brane at $y = 0$ and $y = L$.

$$\begin{aligned}
V(\eta\Phi) &= \lambda_1^{\eta\Phi}(\eta^\dagger\eta)_1(\Phi^\dagger\Phi) + \lambda_2^{\eta\Phi}[(\eta^\dagger\Phi)(\Phi^\dagger\eta)]_1 \\
&+ \{\lambda_3^{\eta\Phi}[(\eta^\dagger\Phi)(\eta^\dagger\Phi)]_1 + \text{H.c.}\} \\
&+ \{\lambda_4^{\eta\Phi}(\eta^\dagger\eta)_{3_s}(\eta^\dagger\Phi) + \text{H.c.}\} \\
&+ \{\lambda_5^{\eta\Phi}(\eta^\dagger\eta)_{3_a}(\eta^\dagger\Phi) + \text{H.c.}\}.
\end{aligned} \tag{A6}$$

Here μ_η , μ_Φ , μ_χ , ξ_1^χ and ξ_2^χ have mass dimension-1, while $\lambda_{1,\dots,5}^\eta$, λ^Φ , $\lambda_{1,\dots,5}^\chi$ and $\lambda_{1,\dots,5}^{\eta\Phi}$ are

dimensionless. In $V(\eta\Phi)$ the usual mixing term $\Phi^\dagger\eta$ is forbidden by the A_4 symmetry. In the scalar potential (A1)–(A7) we have for simplicity assumed that CP is conserved, and the couplings $\lambda_3^{\eta\Phi}$, $\lambda_4^{\eta\Phi}$ and $\lambda_5^{\eta\Phi}$ are real.

The vacuum configuration is obtained by the vanishing of the derivative of V with respect to each component of the scalar fields Φ , η_i , χ_i ($i = 1, 2, 3$). The vacuum alignment of the field η is determined by

$$\begin{aligned}
\sqrt{2} \frac{\partial V}{\partial \eta_1^0} \Big|_{\langle \eta_i^0 \rangle = v_{\eta_i}} &= \frac{v_{\eta_1}}{2} \{2v_{\eta_1}^2(\lambda_1^\eta + \lambda_2^\eta) + 2\mu_\eta^2 + (v_{\eta_2}^2 + v_{\eta_3}^2)(2\lambda_1^\eta - \lambda_2^\eta + 4\lambda_3^\eta) + v_\Phi^2(\lambda_1^{\eta\Phi} + \lambda_2^{\eta\Phi} + 2\lambda_3^{\eta\Phi})\} \\
&+ 3v_{\eta_2}v_{\eta_3}v_\Phi\lambda_4^{\eta\Phi} = 0, \\
\sqrt{2} \frac{\partial V}{\partial \eta_2^0} \Big|_{\langle \eta_i^0 \rangle = v_{\eta_i}} &= \frac{v_{\eta_2}}{2} \{2v_{\eta_2}^2(\lambda_1^\eta + \lambda_2^\eta) + 2\mu_\eta^2 + (v_{\eta_1}^2 + v_{\eta_3}^2)(2\lambda_1^\eta - \lambda_2^\eta + 4\lambda_3^\eta) + v_\Phi^2(\lambda_1^{\eta\Phi} + \lambda_2^{\eta\Phi} + 2\lambda_3^{\eta\Phi})\} \\
&+ 3v_{\eta_1}v_{\eta_3}v_\Phi\lambda_4^{\eta\Phi} = 0, \\
\sqrt{2} \frac{\partial V}{\partial \eta_3^0} \Big|_{\langle \eta_i^0 \rangle = v_{\eta_i}} &= \frac{v_{\eta_3}}{2} \{2v_{\eta_3}^2(\lambda_1^\eta + \lambda_2^\eta) + 2\mu_\eta^2 + (v_{\eta_1}^2 + v_{\eta_2}^2)(2\lambda_1^\eta - \lambda_2^\eta + 4\lambda_3^\eta) + v_\Phi^2(\lambda_1^{\eta\Phi} + \lambda_2^{\eta\Phi} + 2\lambda_3^{\eta\Phi})\} \\
&+ 3v_{\eta_1}v_{\eta_2}v_\Phi\lambda_4^{\eta\Phi} = 0.
\end{aligned} \tag{A8}$$

From this set of three equations, we obtain the solution

$$\langle \eta_1^0 \rangle = \langle \eta_2^0 \rangle = \langle \eta_3^0 \rangle \equiv v_\eta = \frac{-3v_\Phi\lambda_4^{\eta\Phi} \pm \sqrt{9v_\Phi^2\lambda_4^{\eta\Phi 2} - 2(3\lambda_1^\eta + 4\lambda_3^\eta)(2\mu_\eta^2 + v_\Phi^2(\lambda_1^{\eta\Phi} + \lambda_2^{\eta\Phi} + 2\lambda_3^{\eta\Phi}))}}{2(3\lambda_1^\eta + 4\lambda_3^\eta)} \neq 0. \tag{A9}$$

This VEV breaks A_4 down to a residual Z_3 .

The vanishing of the derivative of V with respect to Φ reads

$$\sqrt{2} \frac{\partial V}{\partial \Phi^0} \Big|_{\langle \Phi^0 \rangle = v_\Phi} = v_\Phi \left\{ v_\Phi^2 \lambda^\Phi + \mu_\Phi^2 + \frac{1}{2}(\lambda_1^{\eta\Phi} + \lambda_2^{\eta\Phi} + 2\lambda_3^{\eta\Phi})(v_{\eta_1}^2 + v_{\eta_2}^2 + v_{\eta_3}^2) \right\} + 3v_{\eta_1}v_{\eta_2}v_{\eta_3}\lambda_4^{\eta\Phi} = 0. \tag{A10}$$

The real-valued solution of Eq. (A10), for real-valued parameters, is

$$v_\Phi = \frac{-\left(\frac{2}{3}\right)^{1/3}\tilde{b}}{\{-9\tilde{a}^2\tilde{c} + \sqrt{3(4\tilde{a}^3\tilde{b}^3 + 27\tilde{a}^4\tilde{c}^2)}\}^{1/3}} + \frac{\{-9\tilde{a}^2\tilde{c} + \sqrt{3(4\tilde{a}^3\tilde{b}^3 + 27\tilde{a}^4\tilde{c}^2)}\}^{1/3}}{\tilde{a}(18)^{1/3}}, \tag{A11}$$

where $\tilde{a} = \lambda^\Phi$, $\tilde{b} = \mu_\Phi^2 + \frac{3}{2}v_\eta^2(\lambda_1^{\eta\Phi} + \lambda_2^{\eta\Phi} + 2\lambda_3^{\eta\Phi})$ and $\tilde{c} = 3v_\eta^3\lambda_4^{\eta\Phi}$.

Finally, the minimization equations for the vacuum configuration of χ are given by

$$\begin{aligned}
\frac{\partial V}{\partial \chi_1} \Big|_{\langle \chi_i \rangle = v_{\chi_i}} &= 2v_{\chi_1}(\mu_\chi^2 + (2\lambda_1^\chi - \lambda_2^\chi + 4\lambda_3^\chi)(v_{\chi_2}^2 + v_{\chi_3}^2) + 2(\lambda_1^\chi + \lambda_2^\chi)v_{\chi_1}^2) + 6\xi_1^\chi v_{\chi_2}v_{\chi_3} = 0, \\
\frac{\partial V}{\partial \chi_2} \Big|_{\langle \chi_i \rangle = v_{\chi_i}} &= 2v_{\chi_2}(\mu_\chi^2 + (2\lambda_1^\chi - \lambda_2^\chi + 4\lambda_3^\chi)(v_{\chi_1}^2 + v_{\chi_3}^2) + 2(\lambda_1^\chi + \lambda_2^\chi)v_{\chi_2}^2) + 6\xi_1^\chi v_{\chi_1}v_{\chi_3} = 0, \\
\frac{\partial V}{\partial \chi_3} \Big|_{\langle \chi_i \rangle = v_{\chi_i}} &= 2v_{\chi_3}(\mu_\chi^2 + (2\lambda_1^\chi - \lambda_2^\chi + 4\lambda_3^\chi)(v_{\chi_1}^2 + v_{\chi_2}^2) + 2(\lambda_1^\chi + \lambda_2^\chi)v_{\chi_3}^2) + 6\xi_1^\chi v_{\chi_1}v_{\chi_2} = 0.
\end{aligned} \tag{A12}$$

From these equations, we obtain the solution⁶

⁶There exists another nontrivial solution $\langle \chi \rangle = v_\chi(1, 1, 1)$ with $v_\chi = \frac{-3\xi_1^\chi \pm \sqrt{9\xi_1^{\chi 2} - 8\mu_\chi^2(3\lambda_1^\chi + 4\lambda_3^\chi)}}{4(3\lambda_1^\chi + 4\lambda_3^\chi)}$. But this solution is not of interest for our purposes.

$$\langle \chi_1 \rangle \equiv v_\chi = \sqrt{\frac{-\mu_\chi^2}{2(\lambda_1^\chi + \lambda_2^\chi)}} \neq 0, \quad \langle \chi_2 \rangle = \langle \chi_3 \rangle = 0. \quad (\text{A13})$$

APPENDIX B: PARAMETRIZATION OF THE NEUTRINO MASS MATRIX

We parametrize the Hermitian matrix $m_\nu m_\nu^\dagger$ as follows:

$$m_\nu m_\nu^\dagger = m_0^2 \begin{pmatrix} \tilde{A} y_1^2 & y_1 y_2 \left(\frac{3Q-P}{2} - i \frac{3(R-S)}{2} \right) & y_1 \left(-\frac{3Q+P}{2} - i \frac{3(R+S)}{2} \right) \\ y_1 y_2 \left(\frac{3Q-P}{2} + i \frac{3(R-S)}{2} \right) & y_2^2 \left(F + G + \frac{9K}{4} + \frac{3D}{2} \right) & y_2 \left(F + G - \frac{9K}{4} - i \frac{3Z}{2} \right) \\ y_1 \left(-\frac{3Q+P}{2} + i \frac{3(R+S)}{2} \right) & y_2 \left(F + G - \frac{9K}{4} + i \frac{3Z}{2} \right) & F + G + \frac{9K}{4} + \frac{3D}{2} \end{pmatrix}.$$

All parameters appearing here are real, and equal to

$$\begin{aligned} \tilde{A} &= 1 + y_1^2 + y_2^2 + \frac{1 + 4y_1^2 + y_2^2}{a^2} - \frac{2(1 - 2y_1^2 + y_2^2) \cos \psi_1}{a}, & K &= \frac{1 + y_2^2}{b^2}, & F &= 1 + y_1^2 + y_2^2 + \frac{1 + 4y_1^2 + y_2^2}{4a^2}, \\ G &= \frac{(1 - 2y_1^2 + y_2^2) \cos \psi_1}{a}, & D &= (1 - y_2^2) \frac{\cos \psi_{12} + 2a \cos \psi_2}{ab}, & Z &= (1 - y_2^2) \frac{\sin \psi_{12} - 2a \sin \psi_2}{ab}, \\ P &= \frac{1 + 4y_1^2 + y_2^2}{a^2} - 2(1 + y_1^2 + y_2^2) + \frac{(1 - 2y_1^2 + y_2^2) \cos \psi_1}{a}, & Q &= (1 - y_2^2) \frac{\cos \psi_{12} - a \cos \psi_2}{ab}, \\ S &= (1 - y_2^2) \frac{\sin \psi_{12} + a \sin \psi_2}{ab}, & R &= \frac{(1 - 2y_1^2 + y_2^2) \sin \psi_1}{a}. \end{aligned} \quad (\text{B1})$$

In Eq. (60) the parameters Ψ_1, Ψ_2 are defined by

$$\begin{aligned} \Psi_1 &= c_{13}^2 y_1^2 \tilde{A} + s_{13}^2 \left\{ \left(F + G + \frac{9K}{4} + \frac{3D}{2} \right) (c_{23}^2 + y_2^2 s_{23}^2) + y_2 \left(F + G - \frac{9K}{4} \right) \sin 2\theta_{23} \right\} - \frac{y_1}{2} \sin 2\theta_{13} \{ 3c_{23} (R + S) \sin \delta_{CP} \\ &\quad - (3Q + P) \cos \delta_{CP} + y_2 s_{23} (3(R - S) \sin \delta_{CP} + (3Q - P) \cos \delta_{CP}) \} \\ \Psi_2 &= \left(F + G + \frac{9K}{4} + \frac{3D}{2} \right) (s_{23}^2 + y_2^2 c_{23}^2) - y_2 \left(F + G - \frac{9K}{4} \right) \sin 2\theta_{23}. \end{aligned} \quad (\text{B2})$$

-
- [1] K. Nakamura *et al.* (Particle Data Group), *J. Phys. G* **37**, 075021 (2010) and 2011 partial update for the 2012 edition.
- [2] P. F. Harrison, D. H. Perkins, and W. G. Scott, *Phys. Lett. B* **530**, 167 (2002); Z. Z. Xing, *Phys. Lett. B* **533**, 85 (2002); P. F. Harrison and W. G. Scott, *Phys. Lett. B* **535**, 163 (2002); X. G. He and A. Zee, *Phys. Lett. B* **560**, 87 (2003).
- [3] F. P. An *et al.* (DAYA-BAY Collaboration), *Phys. Rev. Lett.* **108**, 171803 (2012).
- [4] J. K. Ahn *et al.* (RENO Collaboration), *Phys. Rev. Lett.* **108**, 191802 (2012).
- [5] K. Abe *et al.* (T2K Collaboration), *Phys. Rev. Lett.* **107**, 041801 (2011); P. Adamson *et al.* (MINOS Collaboration), *Phys. Rev. Lett.* **107**, 181802 (2011); H. De Kerret *et al.* (Double Chooz Collaboration), *Sixth International Workshop on Low Energy Neutrino Physics* (Seoul National University, Seoul, 2011).
- [6] R. Nichol, *Neutrino 2012 conference*, <http://neu2012-kek.jp/>.
- [7] M. Tortola, J. W. F. Valle, and D. Vanegas, [arXiv:1205.4018](https://arxiv.org/abs/1205.4018).
- [8] H. Nunokawa, S. J. Parke, and J. W. F. Valle, *Prog. Part. Nucl. Phys.* **60**, 338 (2008).
- [9] Y. H. Ahn, H.-Y. Cheng, and S. Oh, *Phys. Rev. D* **83**, 076012 (2011); Y. H. Ahn, C. S. Kim, and S. Oh, *Phys. Rev. D* **86**, 013007 (2012); Y. H. Ahn, H.-Y. Cheng, and S. Oh, *Phys. Lett. B* **715**, 203 (2012); *Phys. Rev. D* **84**, 113007 (2011); Y. H. Ahn and H. Okada, *Phys. Rev. D* **85**, 073010 (2012); S. Zhou, [arXiv:1205.0761](https://arxiv.org/abs/1205.0761); S. Antusch, C. Gross, V. Maurer, and C. Sluka, [arXiv:1205.1051](https://arxiv.org/abs/1205.1051); G. Altarelli, F. Feruglio, and L. Merlo, [arXiv:1205.5133](https://arxiv.org/abs/1205.5133).
- [10] Y. H. Ahn and S. K. Kang, [arXiv:1203.4185](https://arxiv.org/abs/1203.4185).
- [11] K. S. Babu, E. Ma, and J. W. F. Valle, *Phys. Lett. B* **552**, 207 (2003).
- [12] G. Altarelli and F. Feruglio, *Nucl. Phys.* **B720**, 64 (2005).

- [13] X. G. He, Y. Y. Keum, and R. R. Volkas, *J. High Energy Phys.* **04** (2006) 039.
- [14] S. Baek and M. C. Oh, *Phys. Lett. B* **690**, 29 (2010);
- [15] E. Ma and G. Rajasekaran, *Phys. Rev. D* **64**, 113012 (2001).
- [16] T. Fukuyama and H. Nishiura, [arXiv:hep-ph/9702253](https://arxiv.org/abs/hep-ph/9702253); R. N. Mohapatra and S. Nussinov, *Phys. Rev. D* **60**, 013002 (1999); E. Ma and M. Raidal, *Phys. Rev. Lett.* **87**, 011802 (2001); C. S. Lam, *Phys. Lett. B* **507**, 214 (2001); T. Kitabayashi and M. Yasue, *Phys. Rev. D* **67**, 015006 (2003); W. Grimus and L. Lavoura, *Phys. Lett. B* **572**, 189 (2003); **572**, 189 (2003); Y. Koide, *Phys. Rev. D* **69**, 093001 (2004); A. Ghosal, [arXiv:hep-ph/0304090](https://arxiv.org/abs/hep-ph/0304090); W. Grimus and L. Lavoura, *J. Phys. G* **30**, 73 (2004); R. N. Mohapatra and W. Rodejohann, *Phys. Rev. D* **72**, 053001 (2005); Y. H. Ahn, S. K. Kang, C. S. Kim, and J. Lee, *Phys. Rev. D* **73**, 093005 (2006); Y. H. Ahn, S. K. Kang, C. S. Kim, and J. Lee, *Phys. Rev. D* **75**, 013012 (2007).
- [17] M. Fukugita and T. Yanagida, *Phys. Lett. B* **174**, 45 (1986); G. F. Giudice, A. Notari, M. Raidal, A. Riotto, and A. Strumia, *Nucl. Phys.* **B685**, 89 (2004); W. Buchmuller, P. Di Bari, and M. Plumacher, *Ann. Phys. (N.Y.)* **315**, 305 (2005); A. Pilaftsis and T. E. J. Underwood, *Phys. Rev. D* **72**, 113001 (2005).
- [18] K. M. Case, R. Karplus, and C. N. Yang, *Phys. Rev.* **101**, 874 (1956); P. H. Frampton, T. W. Kephart, and S. Matsuzaki, *Phys. Rev. D* **78**, 073004 (2008).
- [19] G. Altarelli and F. Feruglio, *Nucl. Phys.* **B741**, 215 (2006); I. de Medeiros Varzielas, S. F. King, and G. G. Ross, *Phys. Lett. B* **644**, 153 (2007); G. Altarelli, F. Feruglio, and Y. Lin, *Nucl. Phys.* **B775**, 31 (2007).
- [20] S. Antusch, J. Kersten, M. Lindner, M. Ratz, and M. A. Schmidt, *J. High Energy Phys.* **03** (2005) 024.
- [21] C. Jarlskog, *Phys. Rev. Lett.* **55**, 1039 (1985); D. D. Wu, *Phys. Rev. D* **33**, 860 (1986).
- [22] G. C. Branco, R. Gonzalez Felipe, F. R. Joaquim, I. Masina, M. N. Rebelo, and C. A. Savoy, *Phys. Rev. D* **67**, 073025 (2003).